Phys. Status Solidi C **12**, No. 4–5, 452–455 (2015) / **DOI** 10.1002/pssc.201400132

physica status solidi c
www.pss-c.com
current topics in solid state physics

Investigation of cubic GaN quantum dots grown by the Stranski-Krastanov process

M. Bürger*, **J. K. N. Lindner, D. Reuter, and D. J. As**

Universität Paderborn, Department Physik, Warburger Str. 100, 33098 Paderborn, Germany

Received 5 June 2014, revised 18 December 2014, accepted 5 January 2015
Published online 16 February 2015

Keywords cubic GaN, quantum dots, molecular beam epitaxy

* Corresponding author: e-mail: mbuerger@mail.uni-paderborn.de, Phone: +49 5251 60 5848, Fax: +49 5251 60 5831

We investigate the formation of cubic GaN quantum dots (QDs) on pseudomorphic strained cubic AlN layers on 3C-SiC (001) substrates grown by means of molecular beam epitaxy. Surface morphologies of various QD sizes and densities were obtained from uncapped samples by atomic force microscopy. These results were correlated with similar but capped samples by photoluminescence experiments. The QD density varies by one order of magnitude from ~1x10^{10} cm^{-2} to ~1x10^{11} cm^{-2} as a function of the GaN coverage on the surface. The initial layer thickness for the creation of cubic GaN QDs on cubic AlN was obtained to 1.95 monolayers by a comparison between the experimental results and an analytical model. Our results reveal the strain-driven Stranski-Krastanov growth mode as the main formation process of the cubic GaN QDs.

1 Introduction The growth of GaN QDs has attracted growing interest as they offer large exciton binding energies and large band offsets. These fundamental properties are promising for optoelectronic applications at high temperatures in the quantum information technology, like single photon sources [1].

The main research interest focuses on the naturally stable wurtzite hexagonal GaN (h-GaN) phase of group III-nitrides. However, in h-GaN QDs a Quantum Confined Stark Effect arises by internal piezoelectric and spontaneous polarization fields along the polar [0001] c-direction. As a result, the confined electrons and holes are spatially separated lowering the oscillator strength and increasing the radiative recombination times. This leads to performance limitations of optoelectronic devices containing h-GaN QDs. Depending on the height of h-GaN QDs the recombination times vary from 100 ps to several µs [2]. In the last decade important steps towards the growth and characterization of metastable cubic GaN (c-GaN) QDs embedded in cubic AlN (c-AlN) barriers have been accomplished. The cubic zinc-blende group III-nitrides were grown along the non-polar (001) direction to avoid undesirable internal fields [3-5]. The radiative recombination times for c-GaN QDs are almost independent of their emission energy [6] and can be two orders of magnitude lower compared to their wurtzite counterparts [7, 8]. Furthermore, single photon emission from self-assembled c-GaN QDs has already been observed [9], but the correlation experiments are limited due to background contaminations. Considerable improvements are expected by lowering the c-GaN QD densities.

Since the Stranski-Krastanov (SK) growth mode was published in the late 1930s [10], lots of efforts were undertaken to investigate this strain-driven island formation process in semiconductors by epitaxial techniques like molecular beam epitaxy (MBE) and metal organic chemical vapor deposition (MOCVD). Compared to lithographical techniques or the two-step epitaxy on cleaved surfaces [11], the fabrication of self-assembled QD nanostructures require less technological efforts.

The analysis of self-assembled InAs SK QDs growth on GaAs reveals a density variation from 10^9 dots/cm^2 to 4x10^{10} dots/cm^2 [12]. In case of group II-VI CdSe QDs on ZnSe the density range accessible exceeds one order of magnitude [13]. Comparable results are achieved with h-GaN QDs grown along the [0001] c-direction on h-AlN [14].

In this work, we focus on the self-assembled formation of c-GaN QDs on c-AlN barrier layers. Samples, either uncapped or capped, with varying amount of nominal GaN coverage are grown by MBE. The morphology of uncapped samples are investigated by atomic force microscopy (AFM) experiments and correlated to photoluminescence (PL) results of capped samples. Our results determine the QD size and density to be a function of the deposited amount of GaN and evidence the SK growth mode as the dominating QD formation mechanism. Furthermore transmission electron microscopy (TEM) experiments reveal single c-GaN QDs in overgrown samples.

2 Experimental Our samples were grown by MBE on 10 µm (001) 3C-SiC substrates on top of 500 µm Si [15]. The growth process was performed in a Riber 32 MBE system adapted with standard effusion cells for Ga and Al evaporation. Atomic nitrogen is provided by an Oxford plasma source and the growth process is *in situ* controlled by reflection high energy electron diffraction (RHEED). Prior to the growth the substrate was cleaned by Al flashes at 910 °C substrate temperature [16]. After cooling down the substrate to a growth temperature of 760°C, the growth of a 30 nm c-AlN buffer layer is initiated. Since the c-AlN layer with a lattice constant of a = 4.37 Å [16] is pseudomorphically strained on 3C-SiC (a = 4.36 Å [17]), a lattice mismatch of ~3.2 % between c-GaN (a = 4.50 Å) [18] and the buffer layer enables the creation of self-assembled QDs by the strain-driven SK process. The three dimensional island formation is indicated by a transition from a streaky to a spotty RHEED pattern [5]. Prior to the QD formation a two dimensional layer c-GaN is expected to be deposited in the Frank-Van der Merwe growth mode [19]. To obtain data from the QDs by AFM measurements, the samples are immediately cooled down after the QD formation. For the optical characterization by PL measurements, the QDs are covered by a 30 nm c-AlN cap layer. Details of the c-AlN and c-GaN QD growth procedure with corresponding RHEED patterns are described in [4, 16, 20].

Two sample batches with and without capping were grown. The amount of deposited GaN varies in both series from 2-4 monolayers (MLs). Taking delay times of the shutters and a deposition time of 0.2 ML/s into account, the accuracy of the deposited amount of GaN is estimated to $\pm$ 0.2 MLs. AFM scans were performed using a Nanosurf Mobile S system in contact mode on uncapped samples to obtain the surface morphology. Regarding the PL experiments the capped samples were excited by a frequency quadrupled Nd:YAG CW laser at 266 nm with an output power of 5 mW. The laser spot is focused to ~200 µm diameter to collect ensemble luminescence data from the QDs. A photomultiplier mounted at a Spex 270 M monochromator is utilized for photon detection. For TEM studies at buried c-GaN QDs a JEOL FX2000 microscope was used at 200 keV.

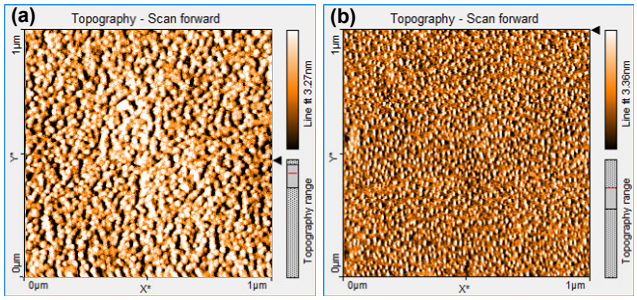

Figure 1 1x1 µm^2 AFM scans of (a) high density QDs (1.2x10^{11} cm^{-2}) and (b) low density QDs (1.5x10^{10} cm^{-2}) formed by 3 MLs and 2 MLs GaN, respectively.

3 Results and discussion

3.1 Atomic force microscopy The surface morphology of two uncapped samples with different amounts of deposited GaN is compared in Fig. 1. The 1x1 µm^2 AFM scan in Fig. 1(a) reveals a high QD density of 1.2x10^{11} cm^{-2}, formed by 3 MLs GaN. The average width of the QDs is ~24 nm with a height of ~2.2 nm. Regarding Fig. 1(b) 2 MLs GaN were deposited resulting in a QD density of 1.5x10^{10} cm^{-2}. The average width and height of the QDs is ~11 nm and ~1.4 nm, respectively. Above 3 ML GaN deposition the coalescence of QDs appears hindering an accurate determination of the QD density and dimensions.

3.2 Photoluminescence spectroscopy To obtain luminescence data from different QD densities, capped samples with 2-4 MLs deposited GaN were investigated. Uncapped c-GaN QDs samples do not show luminescence. Room temperature PL spectra of c-GaN QDs in the range of 3 eV to 4.65 eV are shown in Fig. 2. Due to the delta function like density of states, the optical transitions of QDs are expected to be atom like. With respect to the large number of excited QDs, the observed PL spectra are formed by superimposed individual Gaussian shaped emission bands of many single QDs affected by an unintentional size distribution [21]. The confinement energy of c-GaN QDs in c-AlN leads to transition energies much larger than the band gap energy of bulk c-GaN [22]. The increase of the peak intensity by one order of magnitude with increasing GaN deposition can be attributed to an increase of the QD density within the same range (see Fig. 1). Between 3 and 4 MLs GaN deposition an almost constant peak intensity reveals no significant change in the QD density, but an increase of the QD size (decreasing peak emission energy).

By increasing the amount of deposited GaN, a redshift of the emission energy from 4.25 eV (2 MLs) to 3.56 eV (4 MLs) is observed. This decrease of the emission energy indicates again an increase of the QD size, as obtained by AFM of uncapped QDs (see Fig. 1). Calculations of the exciton transition energy in c-GaN QDs identified the QD height as the main confinement parameter [23]. Further-

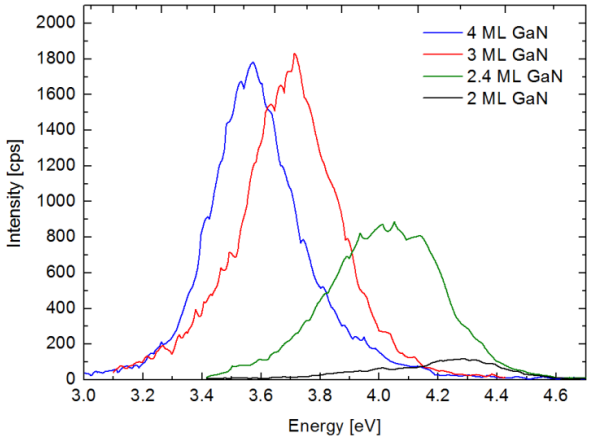

Figure 2 Room temperature PL spectra of c-GaN QDs in the range of 3 eV to 4.65 eV. The amount of nominally deposited GaN is varied from 2-4 MLs corresponding to QD densities from ~1x10^{10} cm^{-2} to ~1x10^{11} cm^{-2}.

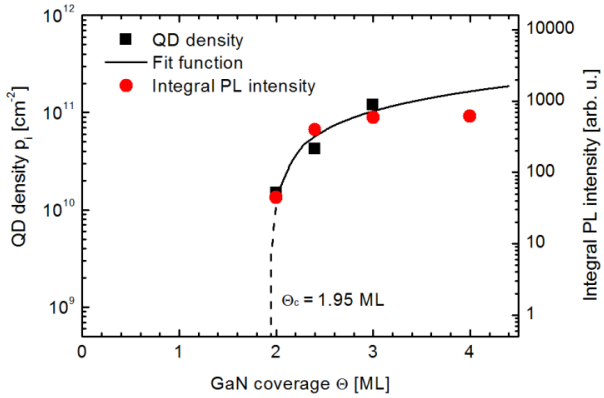

Figure 3 QD density (black squares) as a function of GaN coverage correlated with the integral PL intensities (red dots) from Fig. 1. The QD densities are obtained by AFM scans. The solid line indicates a fit function according to Eq. (1).

more, the redshift of the emission energy agrees with these calculations of the emission energy as a function of the QD height. In the PL spectrum of the 2 MLs GaN sample (black curve) a low energy tail can be observed, which can be caused by a bimodal QD size distribution. It should be mentioned that the high emission energies around 4 eV in Fig. 2 are related to very small QDs, which are close to the resolution limit of AFM (cf. Fig. 1). The Gaussian shaped ensemble emission bands are a superposition of individual QD emission lines and its full-width at half maximum (FWHM) can be used to estimate the QD size distribution [21]. The FWHM decreases from 439 meV (2.4 MLs GaN) to 351 meV (3 MLs GaN) indicating changes in the QD size distribution.

3.3 Critical layer thickness of c-GaN QDs The surface data obtained from AFM scans can be correlated with the PL results. Figure 3 illustrates the analysis of the QD density p_i as a function of the GaN coverage Θ. The AFM data (black squares) and the integral PL intensities (red dots) are plotted versus the amount of deposited GaN in Fig. 3. Both results show an abruptly increase above 2 MLs.

To verify the QD formation mechanism, the experimental data are compared to an analytical model developed by Leonard et al. [12]. This simple empirical model was originally developed for the analysis of self-assembled InAs QDs on GaAs and in the meantime applied to many QD systems. It reveals the SK process as the main formation process and is also suitable to determine the critical layer thickness Θ_c. The QD density p_i is expressed as a function of the surface coverage Θ by

$$p_i = p_0(\Theta - \Theta_c)^{\alpha} . \quad (1)$$

Using $p_0 = 1 \times 10^{11}$ cm^{-2} and an exponent of $\alpha = 0.7$ the model matches reasonably well with the experimental data, as shown by the solid line in Fig. 3 and confirms thereby the formation of self-assembled QDs by the strain-driven SK mechanism. Furthermore, the critical layer thickness Θ_c can be determined to 1.95 MLs (see extrapolated dashed line in Fig. 3.). After reaching the critical layer thickness 3D islands are created to reduce strain and surface energy of the pseudomorphic grown GaN layer [10]. The QD density increases abruptly above Θ_c from ~1x10^{10} cm^{-2} (2 MLs GaN) to ~1x10^{11} cm^{-2} (3 MLs GaN) and agrees with the integral PL intensities. Our results are in good agreement with similar results reported for other semiconductor systems and clearly evidence the formation of QDs by the SK process [12, 13, 14].

It is also worth to mention that many parameters, like the growth temperature, the flux of the deposited material and the growth stoichiometry can influence the shape, size and density distribution of the QDs [14].

3.4 Transmission electron microscopy To gain further insight in capped QDs, an additional sample with a single layer of SK QDs with the amount of 2.4 MLs GaN was grown for TEM imaging. In Fig. 4 a bright-field cross-sectional TEM image of the capped QD layer structure with high magnification is displayed. In the lower part the interface between the 3C-SiC substrate and the c-AlN buffer layer is highlighted by a white dashed line. This interface has been previously analysed by high resolution transmission electron microscopy (HRTEM) and is atomically sharp [24]. Between the c-AlN buffer and cap layer (brighter areas) a thin single layer of c-GaN QDs (dark areas) is apparent. The red rectangle magnifies a single QD in a defect free environment. As a guide for the eyes the white border lines indicate a truncated pyramid shape for the proposed c-GaN QD similar to the shape used for the calculations of the transition energies in Ref. [23]. The dimensions of the QD can be roughly estimated to a diameter of 10-15 nm and to a height of ~1.5 nm. The thickness of the c-AlN layers are measured to ~32 nm.

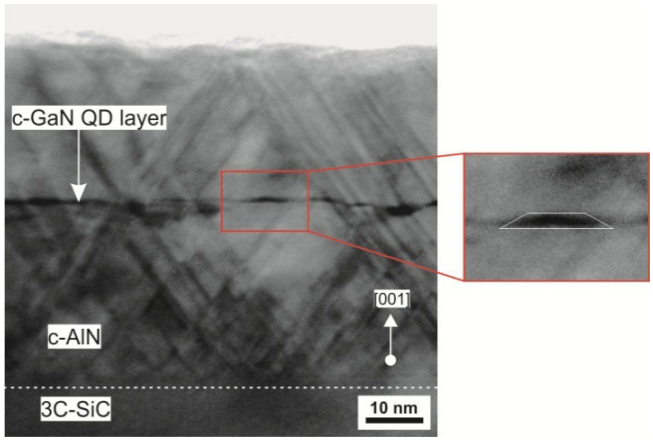

Figure 4 TEM image in cross-section geometry of the active c-AlN/c-GaN QD layer. The red rectangle shows a more detailed image of a single c-GaN QD. The white border lines of the magnified QD shows the assumed QD shape of Ref. [23] as a guide for the eyes.

Stacking faults are extended across the entire active layer without interrupting at the QDs. These bunches of stacking faults on {111} planes (orientated 57.4° towards the (001) sample surface) impose phase shifts of the electron waves and therefore lead to darker stripes. A superposition of strain-induced and material contrast appears at the intersection of stacking faults and the c-GaN QDs and result in extended dark spots. These local strain fields hamper an undisturbed view of the QDs and prevent an accurate determination of the QD dimensions especially in areas with high defect densities. Similar stacking fault distributions have also been observed in TEM studies of multi-quantum well structures which starts with the nucleation of a c-AlN layer on the 3C-SiC substrate [24]. Further investigations by HRTEM shall identify the strain distribution within QDs and reveal the influence of stacking faults on the formation process in detail.

4 Conclusions We investigated c-GaN QDs fabricated by MBE and revealed the SK growth mode as the main mechanism for the QD formation. Density and size distribution of uncapped samples were measured by AFM. The AFM data were correlated with PL results of capped samples. The comparison between the experimental data and an analytical model determined the critical layer thickness of c-GaN QDs on pseudomorphic strained c-AlN on 3C-SiC to 1.95 MLs. Close to the critical thickness it is possible to create QDs with a density as low as ~$1x10^{10}$ cm^{-2}. TEM experiments of c-GaN QDs in a region without stacking faults indicated a truncated pyramid shape for the proposed c-GaN QD and underlines the existence of buried QDs in capped samples.

Acknowledgements This work was supported by the DFG graduate program GRK 1464 “Micro- and Nanostructures in Optoelectronics and Photonics”.

References

[1] C. Santori, D. Fattal, and Y. Yamamoto, Single-photon Devices and Applications (Wiley-VCH, New York, 2010).
[2] S. Kako, M. Miyamura, K. Tachibana, K. Hoshino, and Y. Arakawa, Appl. Phys. Lett. **83**, 984 (2003).
[3] B. Daudin, G. Feuillet, J. Hübner, Y. Samson, F. Widmann, A. Philippe, C. Bru-Chevallier, G. Guillot, E. Bustarret, G. Bentoumi, and A. Deneuville, J. Appl. Phys. **84**, 2295 (1998).
[4] D.J. As, Microelectron. J. **40**, 204 (2009).
[5] T. Schupp, T. Meisch, B. Neuschl, M. Feneberg, K. Thonke, K. Lischka, and D.J. As, AIP Conf. Proc. **1292**, 165 (2010).
[6] S. Sergent, S. Kako, M. Bürger, D.J. As, and Y. Arakawa, Appl. Phys. Lett. **103**, 151109 (2013).
[7] J. Simon, N. T. Pelekanos, C. Adelmann, E. Martinez-Guerrero, R. André, B. Daudin, Le Si Dang, and H. Mariette, Phys. Rev. B **68**, 035312 (2003).
[8] T. Bretagnon, P. Lefebvre, P. Valvin, R. Bardoux, T. Guillet, T. Taliercio, and B. Gil, Phys. Rev. B **73**, 113304 (2006).
[9] S. Kako, M. Holmes, S. Sergent, M. Bürger, D.J. As, and Y. Arakawa, Appl. Phys. Lett. **104**, 011101 (2014).
[10] I.N. Stranski and L. Krastanow, Mon.hft. f. Chem. **71**, 351 (1937).
[11] D. Bimberg, Semiconductor Nanostructures (Springer, Berlin, 2008).
[12] D. Leonard, K. Pond, and P.M. Petroff, Phys. Rev. B **50**, 11687 (1994).
[13] D. Schikora, S. Schwedhelm, D.J. As, K. Lischka, D. Litvinov, A. Rosenauer, D. Gerthsen, M. Strassburg, A. Hoffmann, and D. Bimberg, Appl. Phys. Lett. **76**, 418 (2000).
[14] Y. Arakawa, M. Miyamura, K. Tachibana, K. Hoshino, and S. Kako, Instr. Phys. Conf. Ser. **171**, 61 (2003).
[15] T. Chassagne, A. Leycuras, C. Balloud, P. Arcade, H. Peyre, and S. Juillaguet, Mater. Sci. Forum **457–460**, 273 (2004).
[16] T. Schupp, K. Lischka, and D.J. As, J. Cryst. Growth **312**, 1500 (2010)
[17] A. Taylor and R. M. Jones, Silicon Carbide - A High Temperature Semiconductor, edited by J. R. O'Connor (Pergamon Press, 1960).
[18] S. Strite, J. Ruan , Z. Li, A. Salvador, H. Chen, D. J. Smith, W. J. Choyke, and H. Morko, J. Vac. Sci. Technol. B **9**, 1924 (1991).
[19] F.C. Frank and J.H Van der Merwe, Proc. R. Soc. London, Ser. A **198**, 205 (1949).
[20] M. Bürger, T. Schupp, K. Lischka, and D. J. As, Phys. Status Solidi C **9**, 1273 (2012).
[21] G. Schmid, Nanoparticles: From Theory to Application (Wiley-VCH, New York, 2006).
[22] D. J. As, F. Schmilgus, C. Wang, B. Schöttker, D. Schikora, and K. Lischka, Appl. Phys. Lett. **70**, 1311 (1997).
[23] V. A. Fonoberov and A. A. Balandin, J. Appl. Phys. **94**, 7178 (2003).
[24] R.M. Kemper, C. Mietze, L. Hiller, T. Stauden, J. Pezoldt, D. Meertens, M. Luysberg, D.J. As, and J.K.N. Lindner, Phys. Status Solidi C **11**, 265 (2014).